Ind. J. Pharm. Edu. Res., 2025; 59(3):1067-1077.
https://www.ijper.org

Original Article

Natural Compounds and Their Small Molecule Derivatives as PI3-Kinase Inhibitors against Cancer

Abuzer Ali[1,*], Amena Ali[2]

[1]Department of Pharmacognosy, College of Pharmacy, Taif University, Taif, SAUDI ARABIA.
[2]Department of Pharmaceutical Chemistry, College of Pharmacy, Taif University, Taif, SAUDI ARABIA.

ABSTRACT

Objectives: Earlier findings revealed the importance of different natural compounds and synthetic drugs in the treatment of cancer by targeting Phosphoinositide 3-Kinase (PI3K). In the direction to discover novel PI3K inhibitors, the present study includes the generation of fragment derivatives. Natural compounds and FDA-approved synthetic drugs were selected for screening against PI3K by using different computational methodologies. **Materials and Methods:** The top ranked compounds dehydroglyasperin D, honokiol and quercetin were taken for generation of derivatives and 30 (out of 300) derivatives were screened with less than 2 synthetic accessibility scores. The ADME property predictions were also performed. **Results:** The top ranked derivatives of honokiol (15_Hono-1) and dehydroglyasperin D (40_Dehydro-2) showed the best binding interactions, with docking scores of -10.09 and -8.61 Kcal/mol, respectively. Further, the PASS prediction coefficient with tumor cell lines and non-tumor cell lines showed the importance of derivatives action against tumor. The pharmacophore modeling determined the important interactive sites with receptors and MMGBSA method was used for rescoring of docking poses. Based on the results, honokiol and dehydroglyasperin D derivatives may become efficient lead compounds as PI3K inhibitors against cancer. **Conclusion:** The study is based on the screening of potent compounds as PI3K inhibitors. The screened compound showed similar binding interactions as reference ligand. The screened compounds have drug-likeness properties. The study may be beneficial for researchers in the development of natural compounds as PI3K inhibitors for the treatment of cancer.

Keywords: Cancer, Dehydroglyasperin D, Honokiol, Molecular docking, Phosphoinositide 3-kinase, PI3K inhibitor.

Correspondence:
Dr. Abuzer Ali
Department of Pharmacognosy, College of Pharmacy, Taif University, P.O. Box 11099, Taif-21944, SAUDI ARABIA.
Email: abuali@tu.edu.sa
ORCID ID: 0000-0002-4313-3896

Received: 13-02-2024;
Revised: 27-08-2024;
Accepted: 02-04-2025.

INTRODUCTION

Cancer remains a major concern worldwide after available of different medicines and novel therapies. Cancer is associated with mutation in genes those are involved in normal growth of cells. The treatment of cancer is limited to early stages with the improvement of novel therapies, but metastasized stage cannot be treatable easily. Most of the treatments are expensive and related to severe adverse effects which may be uncomfortable for humans.[1,2] Target therapy becomes an interesting approach for the treatment of cancer which requires specific target based on types of cancer.[3,4] The targeted therapy showed lesser side effects with cost effective techniques. Earlier report showed that different synthetic drugs are used in the treatment of cancer. Furthermore, phytocompounds also used to prevent and cure cancer with lesser side effects.[5] Different intracellular pathways are involved in the regulation of cell proliferation and apoptosis. PI3K/AKT/mTOR signaling is important pathway involved in cancer cell development.[6] Various inhibitors have been developed to target PI3K signaling in which few are under clinical trial studies. There are various PI3k isoforms as class I (PI3K-α, β, δ and γ), class II (PI3KC2-α, β, γ) class III (Vps34) that have role in tumor biology. They are also important to choose proper target for the treatment of specific cancer.[7] The present study describes the role of different natural compounds on inhibition of PI3K signaling pathway.[8] The PI3K shows important role in cell cycle progression, repair of DNA, motility, angiogenesis and cellular metabolism.[9] The PI3K pathway is the most active and selective for cancer treatment among other targeted kinases.[10,11] The activation of PI3Ks changes phosphatidylinositol (3,4)-bisphosphate to phosphatidylinositol (3,4,5)-triphosphate.[12,13] Second messengers responsible for transfer of signal from cell surface to cytoplasm and phosphorylate other substrate to make proliferation, survival and normal growth of cell. It also connects to other pathways that control cell proliferation and growth, such as MAPK. Angiogenesis and carcinogenesis are linked to mutations in the PI3Ks pathway.[14] Depletion of PTEN's regulatory action, amplification of PI3Ks

DOI: 10.5530/ijper.20256422

and mutations in the receptor tyrosine kinase are all causes that contribute to the pathway's aberration.

Drug repurposing becomes a novel strategy in the drug discovery process that is known as therapeutic switching or drug repositioning. In this strategy we can search novel drug candidates with new pharmacological activities on the basis of already available FDA approved drug molecules. The drug discovery process taking a long period with high manpower and cost including risk association can be overcome by drug repositioning with high success of drug development.[15] Thus, PI3k becomes an interesting target for treatment of cancer. Several naturally abundant phytocompounds such as dehydroglyasperin D, honokiol, quercetin, 6- and 10-gingerol, apigenin, di-indolylmethane, curcumin, thymoquinone, resveratrol, emodin, cryptotanshinone, indole 3-carbinol andrographolide, evodiamine, fisetin, tocotrienol and wogonine showed their potential against PI3K.[16] Further, our idea moved in the direction to discover fragment or small molecule derivatives of these compounds as target of PI3K. Furthermore, several synthetic drugs are also available against PI3K such as apitolisib, idelalisib, pictilisib, duvelisib, copanlisib, dactolisib, buparlisib, gedatolisib, alpelisib and taselisib.[17] These synthetic drugs are approved for targeting PI3K.[18] In the present study molecular docking studies were performed in correlation with some other studies on natural compounds and synthetic drugs against PI3K. Best derivatives or small molecules of these phytocompounds were screened by comparing with synthetic drugs. ADME properties determine the drug likeness properties of small molecules or fragment compounds of best docking score natural compounds. The pharmacophore models, CLC-Pred and MMGBSA based methods further used for the identification of potential natural compounds as PI3K inhibitor.

MATERIALS AND METHODS

Finding of ligands

The natural compounds have been selected on the basis of online data search and total 18 compounds were found with PI3K inhibitory activity. These compounds possessed PI3K inhibitory activity but not published for correlation between their inhibitory activities. Furthermore, 12 synthetic drugs have been selected randomly having PI3K inhibitory activity and also selected as reference drug in the following study. These molecules are also included in online database of PubChem (https://pubchem.ncbi.nlm.nih.gov/).[19] The details of the study presented by flow chart depicted in Figure 1. These compounds prepared by ligprep module for energy minimization and conformation generation. The prepared compounds further used for ADME calculation and docking studies.

ADMET prediction of phytocompounds

The drug development strategy includes small molecule as important properties of drug likeliness for producing pharmacological effects. *In vivo* study for majority of drugs is time taken and costly processes that can be minimise by *in silico* studies. In the present study, Schrodinger ADME and pkCSM tools (a graph modeling-based tool) have been used for calculating ADME properties. SMILEs format has been used for calculating these properties through pkCSM tool (Supplementary materials S1, S2 and S3).[20]

Docking studies of phytocompounds and synthetic drugs against PI3K

In the present work Glide module of Schrodinger software was used as a tool to perform docking study. The binding interactions with target protein depicted in term of binding scores where specific conformer of ligand with lowest energy bind with receptor.[21-28] Pubchem databse used for ligand procurement and converted into mol2 format by using software known as OpenBabel 2.2.3.[29] The protein structure of PI3K (PDB id 3L13) with good resolution was taken in PDB format from protein data bank (RCSB-PDB). The grid size was defined as x, y and z coordinates having size 21.86 for x, 63.45 for y and 20.82 for z. The residue includes SER806, ALA805, MET804, LYS802, THR887, ALA885, TRP812, VAL882, ILE881, GLU880, ILE879, ASP841, LEU838, ASP836, LYS833, ILE831, MET953, PHE961, ILE963, ASP964 AND PHE965. The pH was adjusted to 7+/-2. Theme of the study includes to figure out how natural compounds and synthetic drugs interact with the target protein. The different docking scores make a comparison between different phytocompound against PI3K. These phytocompounds further comprised with synthetic reference drugs for evaluation of their binding interactions (supplementary materials S4 and S5).

Generation of best docked phytocompounds derivatives

The three-top ranked phytocompounds (dehydroglyasperin D, honokiol and quercetin) were used for the generation of derivative compounds by using Ligdream tool (https://www.playmolecule.org/LigDream/) based on deep Neural Networking (DNNs). This tool generates different derivative molecules in excel format having smiles of each compound. DNNs generally used for retrosynthesis in chemical synthesis of compounds.[30] This process further proceeds in the laboratory for the synthesis of target fragments.

ADME properties prediction of small molecule derivatives

SwissADME (http://www.swissadme.ch/) and Schrodinger ADME tool were used for calculating the properties of derivatives of each phytocompound. The selected 3 top ranked phytocompounds screened 100 derivatives from each which

further taken in SwissADME for calculating ADME properties. The smile format of phytocompounds (100 from each category) has been used for determination of ADME properties through SwissADME online tool (http://www.swissadme.ch/). This tool generates drug likeliness properties, cytochrome p450 inhibitory activity and other pharmacokinetic properties. Based on these properties (score of synthetic accessibility and the drug-like behaviour), further 300 derivatives of small molecules screened that showed drug like properties and used for docking purpose (Lipinski/ Ghose/ Veber/ Egan/ Muegge).[31,32] Finally, 22 derivatives were selected from 300 compounds having best properties (supplementary material S3).

Molecular Docking studies of derivatives

Further, docking study was performed on selected derivative compounds using Schrodinger software. The docking scores and binding free energy (ΔG) were calculated for each molecule using same methodologies as described for phytocompounds and reference drugs (supplementary material S6).

MMGBSA

The prime MMGBSA method exhibited the relative binding-free energy (ΔG bind) of each ligand molecule. Binding-free energy, Δ*Gbind*, of a molecular system was calculated as follows.[33]

$$\Delta G(bind)=\Delta G(solv)+\Delta E(MM)+\Delta G(SA)$$

Where, ΔGsolv represents the energy difference between inhibitor complex with receptor and unliganded receptor. ΔEMM represents the minimized energy difference between inhibitor and sum of the energy of unliganded receptor. ΔGSA represents the difference in surface area energies. Prime MM-GBSA calculates the energy of optimized free receptors, free ligand and a complex of the ligand with a receptor.

Cytotoxicity prediction

Cytotoxicity prediction determines the effect of compounds on different cell lines by *in silico* studies. An online tool Cell Line Cytotoxicity Predictor (CLC-Pred) has been used for the study. Prediction of Activity Spectra for Substances (PASS) used for the building of cell line virtually. The structural properties responsible for prediction of cytotoxicity on different cell lines. Both *in vivo* experiments and *in silico* prediction results look similar to maximum value.[34] To predict the cytotoxic effects a website htt p://www.way2drug.com/Cell-line/ was utilized. CLC-Pred tool assume that any compound should be taken for experimental study or not. Here 'Pa' designate to activity and 'Pi' assumes for inactivity. The parameter Pa > Pi action probability should be higher than inactivity probability.

Development of Pharmacophore

Development of pharmacophore was performed by Zinc Pharmer Pharmacophore tool (zincpharmer.csb.pitt.edu). The key properties required for the activity with PDB ID: 3L13 are determined by a pharmacophore study. It can be generated by ligand or structure-based methods.[32,35] The ligand-based method has been used in the present study for the development of pharmacophore where two potent compounds were chosen from the study. In the present study, four chemical features were selected to generate the pharmacophore model including hydrogen bond Acceptor (A), hydrogen bond Donor (D), Hydrophobic (H) and aromatic Ring (R) with the different ligands. These structures were taken from the derivatives of phytocompound dehydroglyasperin D and honokiol.

RESULTS

Drug candidates are measured with different parameters such as safety and efficacy before FDA approval. The ADME property is a best way to find out these parameters though *in silico* methods. The different parameters of ADME properties of the phytocompounds and synthetic drugs are described in Table 1. The water solubility at 25°C of different molecules was also determined. The phytocompounds dehydroglyasperin D, honokiol and quercetin showed good solubility and intestinal absorption as compared with synthetic drugs (Table 1).

Docking interactions of phytocompounds and reference drugs

Molecular docking study for synthetic reference drugs such as apitolisib, idelalisib, pictilisib, duvelisib, copanlisib, dactolisib, buparlisib, gedatolisib, alpelisib, taselisib and selected natural compounds: dehydroglyasperin D, honokiol, quercetin, 10-gingerol, apigenin, di-indolylmethane, curcumin, thymoquinone, resveratrol, 6-gingerol, emodin, cryptotanshinone, indole 3-carbinol andrographolide, evodiamine, fisetin, tocotrienol and wogonin, described the interactions with target protein PI3K. The identification of interactions involved in docking studies of synthetic pharmaceuticals drugs and natural compounds with the target protein PI3K revealed that the most phytocompounds have good docking scores comparable to reference drugs. However, among all compounds and reference drugs, dehydroglyasperin D and honokiol and quercetin showed the best docking scores (Table 2). Compounds having low binding energy confirmed as good docking score and can be taken for further process. Thus, dehydroglyasperin D, honokiol and quercetin were chosen for further study because their binding energies were -10.428 kcal/mol, -9.982 kcal/mol and -10.803 kcal/mol, respectively (Figure 2A and B). Quercetin involved various amino acids for binding interactions in docking study includes TYR867, LYS833, ASP964, VAL882, GLU880, while 10-gingerol showed interactions with ASP950, TYR867 and VAL882 of PI3K (Figure 2B). Synthetic drug apitolisib with binding energy -9.366 Kcal/mol was picked as a reference. Figures 2 A and B show docked ligand molecules with the receptor PI3K, having essential amino acid interactions required for activity.

Dehydroglyasperin D and honokiol bind with the involvement of the polar and non-polar amino acid residues such as TYR867, VAL882, GLU880 and LYS833 of PI3K. The apitolisib binding involved ALA885, VAL882, ASP964 and ASP841 amino acids. Whereas idelalisib showed binding interactions with VAL882, THR887 and ASP836 (Figure 3A). Synthetic drugs pictilisib and duvelisib showed binding interactions with amino acids ASP836, VAL882, THR887 of PI3K (Figure 3B). Our result is comparable and slightly higher than the previous report.[19] Table 3 depicts dehydroglyasperin D, honokiol and quercetin with their docking scores having comparable interactions with amino acids as shown by synthetic drug apitolisib and consequently these three natural compounds were further used to generate small molecule fragment derivatives. Also, dehydroglyasperin D (-10.428 Kcal/mol) and honokiol (-9.982 Kcal/mol) were found to be most potent compounds as compared to other chosen compounds. Crystal Structures of Pan-PI3-Kinase showed the similar interactions as shown by the potent ligands.

Table 1: Parameters of ADMET properties of phytocompounds and synthetic drugs.

Sl. No.	Phytocompounds	WS (log mol/L)	IA (% Absorbed)	VDss (log L/kg)	TC (log ml/min/kg)	AT (Yes/No)	MD (log mg/kg/day)
1	Dehydroglyasperin D	-4.628	95.182	-0.077	0.564	No	0.524
2	Honokiol	-3.364	93.921	0.355	0.428	No	0.48
3	Quercetin	-3.058	80.414	0.221	0.546	No	0.885
4	10-Gingerol	-2.821	93.591	0.017	1.479	No	0.025
5	Apigenin	-3.038	92.37	-0.183	0.615	No	0.045
6	Di-indolylmethane	3.953	97.399	0.412	0.513	Yes	0.275
7	Curcumin	-3.716	88.823	0.134	0.206	No	0.175
8	Thymoquinone	-1.695	97.797	0.019	0.225	NO	0.743
9	Resveratrol	-2.99	89.422	0.073	0.187	YES	-0.171
10	6-gingerol	3.244	92.876	0.044	1.51	NO	0.355
11	Emodin	-2.622	74.579	0.302	0.194	YES	0.231
12	Cryptotanshinone	-4.252	99.09	0.336	0.847	NO	0.356
13	Indole 3-carbinol	-1.628	90.647	0.052	0.54	NO	0.43
14	Andrographolide	-3.051	94.845	-0.487	1.175	NO	-0.212
15	Evodiamine	-4.259	94.741	94.741	0.297	YES	-0.231
16	Fisetin	-2.987	86.711	0.332	0.227	YES	0.779
17	Tocotrienol	-7.99	90.348	0.905	0.976	No	0.628
18	Wogonin	-3.136	98.281	0.036	0.41	No	-0.212
Sl. No.	**Synthetic drugs**	**WS (log mol/L)**	**IA (% Absorbed)**	**VDss (log L/kg)**	**TC (log mL/min/kg)**	**AT (Yes/No)**	**MD (log mg/kg/day)**
1	Apitolisib	-3.124	70.808	0.295	0.702	NO	-0.335
2	Idelalisib	-2.896	-2.896	-0.081	0.59	Yes	0.418
3	Pictilisib	-3.204	86.172	86.172	0.617	No	0.131
4	Duvelisib	-2.892	94.044	-0.026	0.64	Yes	0.452
5	Copanlisib	-3.227	78.789	0.471	0.709	No	0.112
6	Dactolisib	-2.896	93.004	-0.375	0.784	YES	0.373
7	Buparlisib	-5.056	96.147	-0.691	0.101	No	-0.454
8	Gedatolisib	-3.895	84.169	0.784	0.338	NO	-0.178
9	Alpelisib	-4.571	86.234	-0.461	0.033	No	0.027
10	Taselisib	-2.898	84.123	-0.503	0.507	No	0.215

WS: Water solubility; IA: Intestinal absorption; VDss: Volume of distribution (human), TC: Total clearance; AT: AMES Toxicity; MD: Maximum Dosage (human).

Table 2: Comparison of binding energies by SP and XP methodologies of synthetic drugs and phytocompounds.

Phytochemical compounds			Synthetic drugs		
	DS (XP) (Kcal/mol)	DS (SP) (Kcal/mol)		DS (XP) (Kcal/mol)	DS (SP) (Kcal/mol)
Dehydroglyasperin D	-10.428	-5.931	Apitolisib	-9.366	-9.05
Honokiol	-9.982	-7.111	Idelalisib	-8.261	-8.298
Quercetin	-10.803	-6.018	Pictilisib	-7.58	-8.088
10-gingerol	-8.596	-3.152	Duvelisib	-7.119	-7.894
Apigenin	-9.698	-6.185	Copanlisib	-7.082	-7.456
Di-indolylmethane	-7.921	-5.926	Dactolisib	-7.001	-6.58
Curcumin	-9.122	-5.46	Buparlisib	-5.974	-6.497
Thymoquinone	-7.568	-6.776	Gedatolisib	-5.19	-5.52
Resveratrol	-7.524	-7.844	Alpelisib	-5.139	-5.466
6-Gingerol	-7.151	-4.059	Taselisib	-4.335	-4.181
Emodin	-8.295	-5.004			
Cryptotanshinone	-5.892	-7.262			
Indole 3-carbinol	-5.34	-7.166			
Andrographolide	-4.852	-3.44			
Evodiamine	-4.474	-4.462			
Fisetin	-6.653	-5.47			
Tocotrienol	-4.015	-4.599			
Wogonin	-2.722	-5.351			

DS: Docking score.

Screening of derivatives of phytocompounds

Ligdream tool was used for the generation of hundreds of small molecule derivatives of dehydroglyasperin D, honokiol and quercetin (https://www.playmolecule.org/LigDream/). Compounds were chosen on the basis of drug likeness properties and having synthetic accessibility score of 1-2. Each natural compound yielded seven derivative compounds as a result of this screening procedure. From 300 derivatives derived from these three natural compounds, total 22 were screened based on their docking scores. All 22 derivatives thus obtained were again docked with the target PI3K. Table 4 shows the best top derivatives screened based on ADME profile from 100 derivatives generated from each natural compound (supplementary material S3). Based on the docking scores generated, the top compounds screened from the three phytocompounds were redocked with the target PI3K to validate the docking results.

DISCUSSION

In the present study, natural compounds and synthetic drugs against PI3K were screened. Best derivatives or small molecules of these phytocompounds were screened by comparing with synthetic drugs. These natural compounds and synthetic drugs showed potential interaction with PI3K. The dehydroglyasperin D, honokiol, di-indolylmethane, cryptotanshinone, thymoquinone and wogonin were showed good intestinal absorption compared to synthetic drug. The steady states Volume of Distribution (VDss) of the natural compounds (Table 1) were comparable to those of the synthetic drugs. Furthermore, all of the natural compounds showed negative results for AMES toxicity, indicating that they are safe to use in further research. There are four different types of PI3K (α, β, γ, δ). All four Class I PI3K isoforms are highly homologous within the active site and residues which involved at the active site includes Asp841, Tyr867 and Asp836 essential for anticancer activity. The present study describes the compounds having similar binding interaction required for PI3K inhibitory activity.

Molecular docking studies of PI3K with dehydroglyasperin D (Molecule 40_dehydro-2) and honokiol (Molecule 15_hono-1) derivatives showed binding scores of -8.61 Kcal/mol and -10.09 Kcal/mol, respectively (Table 4). The study showed that the Molecule 15_hono-1 made 3 H-bonds (polar) with the PI3K by amino acids residues ASP964, ASP841, ASP836 and the Molecule 40_dehydro-2 made 2 H-bonds (polar) with PI3K by amino acids residues GLU880, VAL882 (Table 5). Table showed parent molecule dehydroglyasperin D made 4 H-bonds (polar) with PI3K by amino acid residues TYR867, VAL882, GLU880, LYS833. Whereas honokiol made 2 H-bonds (polar) with PI3K by amino acid residues GLU880, TYR867. Thus, Molecule 15_hono-1 and Molecule 40_dehydro-2 derivatives showed good

binding interactions with the receptor PI3K comparable to parent dehydroglyasperin D and honokiol (Figure 4A). It described that these two molecules showed best docking scores and required interaction essential for PI3K inhibitory activity. Further, upon comparative analysis the ligand receptor interactions of the derivatives and parent molecule with PI3K revealed 2 to 4 H-bonds (polar) of derivatives in the catalytic region of PI3K, while only 2 to 3 H-bonds (polar) were engaged in the interaction between parent molecule and PI3K.

Molecule 15_hono-1 and Molecule 40_dehydro-2 fragment derivatives were selected for the prediction of biological spectrum by PASS. Out of a maximum probability score of 1, it determines the chance of activity and inactivity for tumor and non-tumor cells. In this, the significant anti-carcinogenic activity was displayed by both Molecule 15_hono-1 and 40_dehydro-2 derivatives against Melanoma with active coefficient of 0.435 and 0.253, respectively (Table 6). On the other hand, these compounds inhibited the proliferation of major carcinoma cell lines, including skin, lung, ovary, breast, brain, blood, pancreas, haematopoietic and lymphoid tissue and colon. These findings suggested a high potential of anti-carcinogenic activity. The activity of the fragment derivatives also sustained the proliferation of embryonic lung fibroblast, foreskin fibroblast and renal proximal tubule epithelial cells, as indicated in Table 7. This investigation confirms the potential role of Molecule 15_hono-1 and 40_dehydro-2 against tumour generation and inflammation.

Pharmacophore modelling describes the important sites of a drug involved in binding with PI3K. In this study, Molecule 15_hono-1 and 40_dehydro-2 derivative ligands showed different pharmacophore sites for having drug likeliness properties. The 15 hono-1 derivative pharmacophore model revealed pharmacophore sites with one hydrogen bond acceptor, one donor and 1 hydrophobic interaction, which is a key characteristic in drug likeliness properties. Furthermore, Molecule 40_dehydro-2 derivative displayed three hydrogen bond acceptors, two donors and three hydrophobic interactions (Figure 4B). MMGBSA redock methods further used for identification of potential

Table 3: Interactive sites and binding energy with different amino acids of PI3K.

Phytocompounds	ΔG binding energy (Kcal/mol)	Interactive amino acid residues
Dehydroglyasperin D	-43.46	TYR867, VAL882, GLU880, LYS833.
Honokiol	-40.57	GLU880, TYR867.
Quercetin	-50.54	TYR867, ASP964, GLU880, LYS833, VAL882.

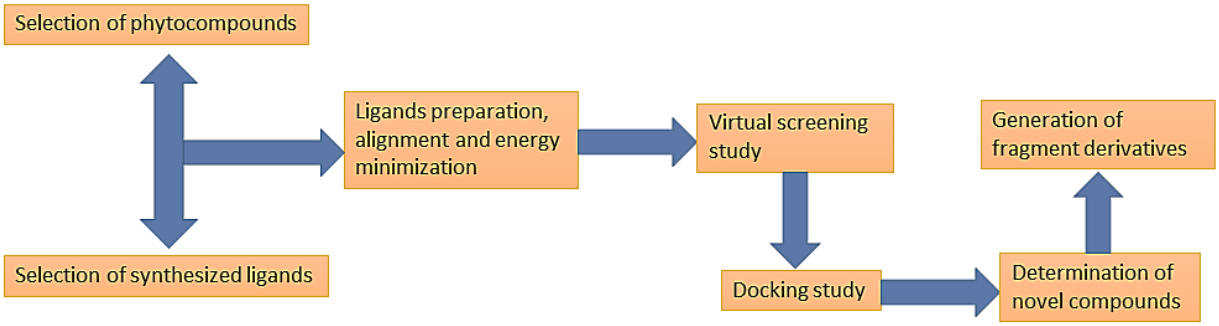

Figure 1: Graphical representation of techniques used in computational study.

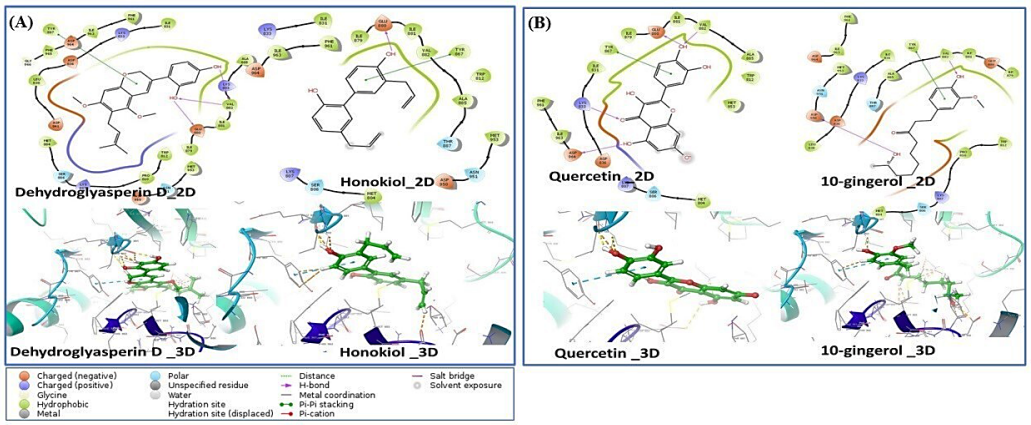

Figure 2: Binding interactions of phytocompounds: (A) dehydroglyasperin 2D with 3D and honokiol 2D with 3D against PI3K; (B) quercetin 2D with 3D and 10-gingerol 2D with 3D against PI3K.

Table 4: ADME properties of derivatives of dehydroglyasperin D, honokiol and quercetin.

Sl. No.	Derivative molecule	DS	MW	QlogPo/w	PSA	PHOA	QPPCaco	QPPMDCK	QPlogBB	QPlogKp	QPlogKhsa
1	15_Hono-1	-10.09	251.33	3.04	35.70	94.47	600.33	315.28	-0.04	-3.14	0.19
2	40_Dehydro-2	-8.61	350.78	3.06	85.21	94.11	564.41	966.35	-0.81	-2.77	0.07
3	63_Que-1	-7.42	295.30	1.91	114.7	62.43	22.73	10.53	-1.67	-4.28	-0.23
4	48_Que-1	-7.25	311.26	3.43	64.62	100.00	1184.51	2743.60	-0.28	-2.21	0.21
5	57_Hono-1	-7.09	286.32	4.21	37.93	100.00	1645.62	1979.44	-0.34	-1.83	0.52
6	49_Hono-1	-6.89	212.25	2.29	55.58	92.88	860.60	420.61	-0.64	-2.55	0.00
7	64_Que-1	-6.91	285.28	2.04	86.44	82.67	280.22	215.88	-1.02	-3.38	-0.03
8	7_Que-1	-6.84	302.28	3.22	67.72	100.00	1142.84	1663.19	-0.36	-2.10	0.18
9	46_Dehy-1	-6.38	348.32	3.64	62.36	100.00	1749.91	4421.62	-0.09	-2.05	0.23
10	7_Que-2	-6.67	302.28	3.16	67.09	100.00	1068.04	1542.51	-0.38	-2.18	0.17
11	64_Que-2	-7.06	285.28	2.02	85.20	83.26	306.94	239.63	-0.97	-3.31	-0.04
12	3_Dehy-1	-5.80	351.74	4.49	48.97	100.00	3595.83	10000.00	0.11	-0.94	0.36
13	6_Que-1	-5.33	318.30	4.36	48.43	100.00	2342.94	6414.26	0.12	-1.79	0.57
14	32_Hono-1	-5.18	219.33	3.71	18.89	100.00	6965.49	4031.63	0.13	-1.00	0.32
15	65_Hono-1	-4.93	313.79	4.25	50.04	100.00	2972.31	3947.67	0.01	-1.18	0.49
16	40_Dehydro-1	-4.98	350.78	3.14	83.98	95.74	653.83	1162.27	-0.75	-2.60	0.10
17	47_Dehy-1	-4.36	348.32	3.66	64.75	100.00	1402.55	3682.74	-0.18	-2.26	0.26
18	42_Dehy-1	-4.36	355.39	2.62	94.19	90.71	507.34	237.58	-1.07	-2.76	0.00
19	63_Que-2	-6.78	295.30	1.71	114.5	61.30	23.01	10.67	-1.64	-4.28	-0.31
20	96_Que-1	-3.87	288.25	2.44	72.92	90.57	569.25	804.80	-0.62	-2.90	-0.01
21	32_Hono-2	-4.69	219.33	3.95	18.58	100.00	6633.67	3824.45	0.10	-1.00	0.42
22	96_Que-2	-4.52	288.25	2.47	72.29	91.84	656.66	942.99	-0.55	-2.76	-0.02

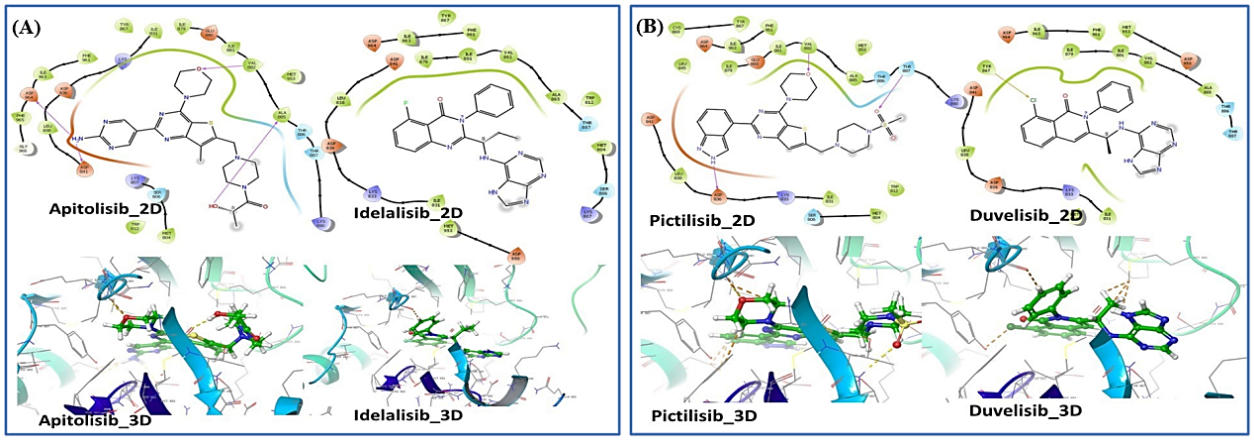

Figure 3: Binding interactions of synthetic compounds: (A) apitolisib 2D with 3D and idelalisib 2D with 3D against PI3K; (B) pictilisib 2D with 3D and duvelisib 2D with 3D against PI3K.

Table 5: Interactive sites and binding energy with different amino acid of PI3k - Molecule 15_hono-1 and Molecule 40_dehydro-2.

Derivative compounds	MMGBSA (ΔG binding energy) (Kcal/mol)	Interactive amino acid residues
Molecule 15_hono-1	-30.59	ASP964, ASP841, ASP836.
Molecule 40_dehydro-2	-40.97	GLU880, VAL882.

natural compound as PI3K inhibitor. The Molecule 15_hono-1 showed ΔG binding energy -30.59 kcal/mol, whereas Molecule 40_dehydro-2 showed -40.97 kcal/mol. These compounds showed good binding energy for the interaction with receptor. The MMGBSA scores of both compounds further compared with standard drug. The standard drug showed ΔG binding energy -32.93 kcal/mol which was comparable with the ΔG binding energies of Molecule 15_hono-1 and Molecule 40_dehydro-2.

ADME properties determine the potential of drug to produce its biological effects by introducing in the body with an appropriate concentration. Molecule 15_hono-1 and 40_dehydro-2 both showed good gut-blood barrier permeability (QPPCaco) with the value 600.33 and 564.41 nm s^{-1} (standard value greater than 500 best), respectively. Blood brain partition coefficient (QPlogBB) values were also observed good for both molecules with -0.04 and -0.81 (standard range -3.0 to -1.2), consecutively. While mimic for the blood brain barrier via MDCK cells (QPPMDCK) showed values 315.28 and 966.35, respectively for both the molecules (standard range of greater than 500 for best compounds). However, skin permeability (QPlogKp) values were observed for both the molecules as -3.14 and -2.77 respectively, within the range of standard values. Both the molecules showed prediction

Table 6: Cytotoxicity prediction on tumor cell lines by phytocompound derivatives showed best binding interaction.

Derivative	Pa*	Pi*	Cell line	Cell line name full	Tissue
Molecule 15_hono-1	0.435	0.037	A2058	Melanoma	Skin
	0.422	0.031	PC-9	Lung adenocarcinoma	Lung
	0.368	0.037	PA-1	Ovarian carcinoma	Ovarium
	0.345	0.013	5637	Urothelial bladder carcinoma	Urinary tract
	0.40	0.097	MDA-MB-453	Breast adenocarcinoma	Breast
	0.333	0.053	T98G	Glioblastoma	Brain
	0.276	0.043	NCI-H69	Small cell lung carcinoma	Lung
	0.263	0.089	NCI-H1299	Non-small cell lung carcinoma	Lung
	0.177	0.014	CEM/C2	Camptothecin-resistant CEM	Blood
	0.18	0.033	BXPC-3	Pancreatic adenocarcinoma	Pancreas
	0.183	0.038	U-937	Histiocytic lymphoma	Haematopoietic and lymphoid tissue.
	0.269	0.127	HT-29	Colon adenocarcinoma	Colon
	0.182	0.05	Ramos	Burkitts lymhoma B-cells	Blood
	0.318	0.196	Hs 683	Oligodendroglioma	Brain
	0.238	0.126	LS174T	Colon adencocarcinoma	Colon
Molecule 40_dehydro-2	0.295	0.062	CCRF-CEM	Childhood T-cell acute lymphoblastic leukemia	Blood
	0.24	0.071	COLO 205	Colon adenocarcinoma	Colon
	0.196	0.056	Jurkat	Acute leukemic T-cells	Blood
	0.26	0.132	HuP-T3	Pancreatic adenocarcinoma	Pancreas
	0.28	0.168	SJSA-1	Osteosarcoma	Bone
	0.199	0.145	HCC 2998	Colon adenocarcinoma	Colon
	0.16	0.106	SAOS-2	Osteosarcoma	Bone
	0.072	0.038	SK-HEP1	Hepatocellular carcinoma	Liver
	0.097	0.076	THP-1	Acute monocytic leukemia	Blood
	0.108	0.089	BT-474	Breast ductal carcinoma	Breast
	0.063	0.046	SW1353	Bone chondrosarcoma	Bone
	0.126	0.11	A-375	Malignant melanoma	Skin
	0.253	0.238	A2058	Melanoma	Skin
	0.183	0.169	MDA-MB-468	Breast adenocarcinoma	Breast
	0.071	0.062	Ishikawa	Endometrial adenocarcinoma	Uterus
	0.07	0.065	TSU	Prostatic carcinoma	Prostate

Table 7: PASS prediction coefficient with non-tumor cell lines by phytocompound derivatives showed best binding interaction.

Derivative	Pa*	Pi*	Cell line	Cell line name	Tissue
Molecule 15_hono-1	0.188	0.012	IMR-90	Embryonic lung fibroblast	Lung
	0.203	0.106	BJ	Foreskin fibroblast	Foreskin
	0.043	0.011	RPTEC	Renal proximal tubule epithelial cells	Kidney
Molecule 40_dehy ro-2	0.113	0.067	HUVEC	Umbilical vein endothelial cell	Endothelium
	0.099	0.087	WI-38	Embryonic lung fibroblast	Lung
	0.153	0.146	HEK293	Embryonic kidney fibroblast	Kidney

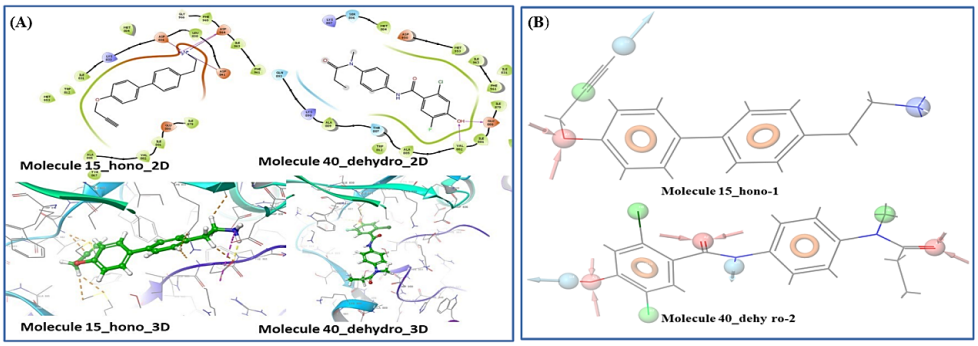

Figure 4: (A) Binding interactions of derivative compounds Molecule 15_hono_2D with 3D and Molecule 40_dehydro_2D with 3D; (B) Pharmacophore model of Molecule 15_hono and Molecule 40_dehydro.

of binding to human serum albumin (QPlogKhsa) with the value of 0.19 and 0.07, respectively (Table 4). Human Oral Absorption value was found good for all compounds. ADME properties were found within the range and supported that the compounds can be used for further developments. ADME properties of the synthetic drug given in supplementary material S7 which was used as standard for the data shown by screened derivatives. The screened compounds were within the limit with the given value and can be used for the generation of future PI3K inhibitors.

CONCLUSION

Even in today's world of advanced science and breakthrough treatment, cancer continues to be one of the leading causes of mortality worldwide. Phytochemicals have been used for decades to prevent and treat a variety of illnesses and recent data suggests the role of phytochemicals in effective cancer treatment. 3D target protein frameworks have played a major role in the design and development of novel or alternative drugs in this area. The top ranked derivatives of honokiol (15_Hono-1) and dehydroglyasperin D (40_Dehydro-2) showed the best binding interactions. Further, the PASS prediction coefficient with tumor cell lines and non-tumor cell lines showed the importance of derivatives action against tumor. The pharmacophore modeling determined the important interactive sites with receptors and MMGBSA method was used for rescoring of docking poses. Based on earlier investigations and the findings presented here, it is proposed that honokiol and dehydroglyasperin D derivatives are efficient lead compounds for combatting PI3K against cancer. However, honokiol (15_Hono-1) revealed as the most potent PI3K inhibitor. The presented *in silico* method might be used to discover the possible applications of a variety of additional natural compounds as well as available FDA approved pharmaceuticals against PI3K.

ACKNOWLEDGEMENT

The authors extend their appreciation to Taif University, Saudi Arabia, for supporting this work through project number (TU-DSPP-2024-43).

FUNDING

This research was funded by Taif University, Saudi Arabia, Project number (TU-DSPP-2024-43).

CONFLICT OF INTEREST

The authors declare that there is no conflict of interest.

ABBREVIATIONS

PI3K: Phosphoinositide 3-kinase; **MAPK:** Mitogen-activated protein kinase; **PTEN:** Phosphatase and tensin homolog on chromosome 10; **FDA:** U.S. Food and Drug Administration; **ADME:** Absorption, distribution, metabolism, excretion; **MMGBSA:** Molecular mechanics with generalised Born and surface area solvation; **PDB:** Protein data bank; **SER806:** Serine; **ALA805:** Alanine; **MET804:** Methionine; **LYS802:** Lysine; **THR887:** Threonine; **TRP812:** Tryptophan; **VAL882:** Valine; **ILE881:** Isoleucine; **GLU880:** Glutamic acid; **ASP841:** Aspartic acid; **LEU838:** Leucine; **PHE961:** Phenylalanine; **TYR867:**

Tyrosine; **DNNs:** Deep Neural Networking; **CLC-Pred:** Cell line cytotoxicity predictor; **DS:** Docking score; **MW:** Molecular weight; **QlogPo/w:** Poctanol/water partition coefficient; **PHOA:** Predicted percent human oral absorption; **QPPCaco:** Predicted Caco-2 cell permeability; **QPPMDCK:** Predicted apparent MDCK cell permeability; **QPlogBB:** Predicted brain/blood partition coefficient; **QPlogKp:** Predicted skin permeability; **QPlogKhsa:** Prediction of human serum albumin binding; **15_Hono-1:** Honokiol; **40_Dehydro-2:** Dehydroglyasperin D.

SUMMARY

The treatment of cancer is limited to early stages with the improvement of novel therapies, but metastasized stage cannot be treatable easily. Various inhibitors have been developed to target PI3K signaling in which few are under clinical trial studies. The present study describes the role of different natural compounds and their small molecule derivatives on inhibition of PI3K signaling pathway. The PI3K shows important role in cell cycle progression, repair of DNA, motility, angiogenesis and cellular metabolism. The PI3K pathway is the most active and selective for cancer treatment among other targeted kinases. Recent data suggests the role of phytochemicals in effective cancer treatment. The anticancer potential of some natural constituents and their small molecule derivatives were investigated in this work. The top ranked compounds dehydroglyasperin D, honokiol and quercetin were taken for generation of derivatives where 30 (out of 300) derivatives were screened with less than 2 synthetic accessibility scores and good ADME properties. Based on earlier investigations and the findings presented here, it is proposed that honokiol and dehydroglyasperin D derivatives are efficient lead compounds for combatting PI3K against cancer. The honokiol (15_Hono-1) and dehydroglyasperin D (40_Dehydro-2) derivatives both came up with significant binding affinity. However, honokiol (15_Hono-1) revealed as the most potent PI3K inhibitor.

REFERENCES

1. Krzyszczyk P, Acevedo A, Davidoff EJ, Timmins LM, Marrero-Berrios I, Patel M, *et al.* The growing role of precision and personalized medicine for cancer treatment. Technology. 2018;6(3-4):79-100. doi: 10.1142/S2339547818300020, PMID 30713991.
2. Falzone L, Salomone S, Libra M. Evolution of cancer pharmacological treatments at the turn of the third millennium. Front Pharmacol. 2018;9:1300. doi: 10.3389/fphar.2018.01300, PMID 30483135.
3. Chakraborty S, Rahman T. The difficulties in cancer treatment. Ecancermedicalscience. 2012;6:ed16. doi: 10.3332/ecancer.2012.ed16, PMID 24883085.
4. Mokhtari RB, Homayouni TS, Baluch N, Morgatskaya E, Kumar S, Das B, *et al.* Combination therapy in combating cancer. Oncotarget. 2017;8(23):38022-43. doi: 10.18632/oncotarget.16723.
5. Zhang YJ, Gan RY, Li S, Zhou Y, Li AN, Xu DP, *et al.* Antioxidant phytochemicals for the prevention and treatment of chronic diseases. Molecules. 2015;20(12):21138-56. doi: 10.3390/molecules201219753, PMID 26633317.
6. Fruman DA, Chiu H, Hopkins BD, Bagrodia S, Cantley LC, Abraham RT. The PI3K pathway in human disease. Cell. 2017;170(4):605-35. doi: 10.1016/j.cell.2017.07.029, PMID 28802037.
7. Thibault B, Ramos-Delgado F, Guillermet-Guibert J. Targeting Class I-II-III PI3Ks in cancer therapy: recent advances in tumor biology and preclinical research. Cancers (Basel). 2023;15(3):784. doi: 10.3390/cancers15030784, PMID 36765741.
8. Reddy L, Odhav B, Bhoola KD. Natural products for cancer prevention: a global perspective. Pharmacol Ther. 2003;99(1):1-13. doi: 10.1016/S0163-7258(03)00042-1, PMID 12804695.
9. Cantley LC. The phosphoinositide 3-kinase pathway. Science. 2002;296(5573):1655-7. doi: 10.1126/science.296.5573.1655, PMID 12040186.
10. Workman P, Clarke PA, Guillard S, Raynaud FI. Drugging the PI3 kinome. Nat Biotechnol. 2006;24(7):794-6. doi: 10.1038/nbt0706-794, PMID 16841064.
11. Clarke PA, Workman P. Phosphatidylinositide-3-kinase inhibitors: addressing questions of isoform selectivity and pharmacodynamic/predictive biomarkers in early clinical trials. J Clin Oncol. 2012;30(3):331-3. doi: 10.1200/JCO.2011.38.7167, PMID 22162582.
12. Okkenhaug K, Vanhaesebroeck B. PI3K in lymphocyte development, differentiation and activation. Nat Rev Immunol. 2003;3(4):317-30. doi: 10.1038/nri1056, PMID 12669022.
13. Yap TA, Bjerke L, Clarke PA, Workman P. Drugging PI3K in cancer: refining targets and therapeutic strategies. Curr Opin Pharmacol. 2015;23:98-107. doi: 10.1016/j.coph.2015.05.016, PMID 26117819.
14. Osaki M, Oshimura M, Ito H. PI3K-Akt pathway: its functions and alterations in human cancer. Apoptosis. 2004;9(6):667-76. doi: 10.1023/B:APPT.0000045801.15585.dd, PMID 15505410.
15. Singh TU, Parida S, Lingaraju MC, Kesavan M, Kumar D, Singh RK. Drug repurposing approach to fight COVID 19. Pharmacol Rep. 2020;72(6):1479-508. doi: 10.1007/s43440-020-00155-6, PMID 32889701.
16. Suvarna V, Murahari M, Khan T, Chaubey P, Sangave P. Phytochemicals and PI3K inhibitors in cancer-an insight. Front Pharmacol. 2017;8:916. doi: 10.3389/fphar.2017.00916, PMID 29311925.
17. Yang J, Nie J, Ma X, Wei Y, Peng Y, Wei X. Targeting PI3K in cancer: mechanisms and advances in clinical trials. Mol Cancer. 2019;18(1):26. doi: 10.1186/s12943-019-0954-x, PMID 30782187.
18. Curigliano G, Shah RR. Safety and tolerability of Phosphatidylinositol-3-Kinase (PI3K) inhibitors in oncology. Drug Saf. 2019;42(2):247-62. doi: 10.1007/s40264-018-0778-4, PMID 30649751.
19. Kaiser J. Science resources. Chemists want NIH to curtail database. Science. 2005;308(5723):774. doi: 10.1126/science.308.5723.774a, PMID 15879180.
20. Pires DE, Blundell TL, Ascher DB. Predicting small-molecule pharmacokinetic properties using graph-based signatures. J Med Chem. 2015;58(9):4066-72. doi: 10.1021/acs.jmedchem.5b00104, PMID 25860834.
21. Morris GM, Huey R, Lindstrom W, Sanner MF, Belew RK, Goodsell DS, *et al.* Autodock4 and AutoDockTools4: automated docking with selective receptor flexibility. J Comput Chem. 2009;30(16):2785-91. doi: 10.1002/jcc.21256, PMID 19399780.
22. Chowdhury P. *In silico* investigation of phytoconstituents from Indian medicinal herb '*Tinospora cordifolia* (giloy)'against SARS-CoV-2 (COVID-19) by molecular dynamics approach. J Biomol Struct Dyn. 2021;39(17):6792-809. doi: 10.1080/07391102.2020.1803968, PMID 32762511.
23. Anant A, Ali A, Ali A, Gupta GD, Asati V. A Computational approach to discover potential quinazoline derivatives against CDK4/6 kinase. J Mol Struct. 2021;1245:131079. doi: 10.1016/j.molstruc.2021.131079.
24. Dhiman S, Saha M, Ali A, Ali A, Gupta GD, Asati V. Structural aspects of triazole derivatives as HSP90 inhibitors for the treatment of cancer: *in silico* studies. J Biomol Struct Dyn. 2023;41(10):4756-69. doi: 10.1080/07391102.2022.2083686, PMID 35665636.
25. Asati V, Bharti SK, Budhwani AK. 3D-QSAR and virtual screening studies of thiazolidine-2,4-dione analogs: validation of experimental inhibitory potencies towards PIM-1 kinase. J Mol Struct. 2017; 1133:278-93. doi: 10.1016/j.molstruc.2016.12.006.
26. Saha M, Gupta S, Dhiman S, Asati V, Ali A, Ali A. Field and atom-based 3D-QSAR models of chromone (1-benzopyran-4-one) derivatives as MAO inhibitors. J Biomol Struct Dyn. 2023;17:1-15. doi: 10.1080/07391102.2023.2166122.
27. Ali A, Ali A. Integrated computational approaches on pyrazoline derivatives as B-Raf kinase inhibitors for the development of novel anticancer agents. J Mol Struct. 2021;1230:129861. doi: 10.1016/j.molstruc.2020.129861.
28. Asati V, Bajaj S, Mahapatra DK, Bharti SK. Molecular modeling studies of some thiazolidine-2,4-dione derivatives as 15-PGDH inhibitors. Med Chem Res. 2016;25(1):94-108. doi: 10.1007/s00044-015-1442-5.
29. O'Boyle NM, Banck M, James CA, Morley C, Vandermeersch T, Hutchison GR. Open Babel: an open chemical toolbox. J Cheminform. 2011;3:33. doi: 10.1186/1758-2946-3-33, PMID 21982300.
30. Ghosh A, Sutradhar S, Baishya D. Delineating thermophilic xylanase from *Bacillus licheniformis* DM5 towards its potential application in xylooligosaccharides production. World J Microbiol Biotechnol. 2019;35(2):34. doi: 10.1007/s11274-019-2605-1, PMID 30706219.
31. Daina A, Michielin O, Zoete V. SwissADME: a free web tool to evaluate pharmacokinetics, drug-likeness and medicinal chemistry friendliness of small molecules. Sci Rep. 2017;7:42717. doi: 10.1038/srep42717, PMID 28256516.
32. Ghosh A, Chakraborty M, Chandra A, Alam MP. Structure-activity relationship (SAR) and molecular dynamics study of withaferin-A fragment derivatives as potential therapeutic lead against main protease (Mpro) of SARS-CoV-2. J Mol Model. 2021;27(3):97. doi: 10.1007/s00894-021-04703-6, PMID 33641023.
33. Gupta S, Baweja GS, Gupta GD, Asati V. Identification of potential N-substituted 5-benzylidenethiazolidine-2, 4-dione derivatives as α-amylase inhibitors: computational cum synthetic studies. J Mol Struct. 2023; 1287:135596. doi: 10.1016/j.molstruc.2023.135596.

34. Lagunin AA, Dubovskaja VI, Rudik AV, Pogodin PV, Druzhilovskiy DS, Gloriozova TA, *et al.* CLC-Pred: A freely available web-service for *in silico* prediction of human cell line cytotoxicity for drug-like compounds. PLOS One. 2018;13(1):e0191838. doi: 10.1371/journal.pone.0191838, PMID 29370280.

35. Wolber G, Seidel T, Bendix F, Langer T. Molecule-pharmacophore superpositioning and pattern matching in computational drug design. Drug Discov Today. 2008;13(1-2):23-9. doi: 10.1016/j.drudis.2007.09.007, PMID 18190860.

Cite this article: Ali A, Ali A. Natural Compounds and Their Small Molecule Derivatives as PI3-Kinase Inhibitors against Cancer. Indian J of Pharmaceutical Education and Research. 2025;59(3):1067-77.